Leaf Area Index estimation in vineyards using a ground-based LiDAR scanner

Jaume Arnó · Alexandre Escolà · Josep M. Vallès · Jordi Llorens · Ricardo Sanz · Joan Masip · Jordi Palacín · Joan R. Rosell-Polo

Jaume Arnó (✉) · Alexandre Escolà · Josep M. Vallès · Ricardo Sanz · Joan Masip · Joan R. Rosell-Polo
Department of Agricultural and Forest Engineering – Research Group on AgroICT and Precision Agriculture, University of Lleida, Rovira Roure, 191, Lleida, 25198, Spain
E-mail: JArno@eagrof.udl.cat
Tel.: +34 973 702 859
Fax: +34 973 702 673
URL: www.grap.udl.cat

Jordi Llorens
Department of Agri Food Engineering and Biotechnology, Politechnical University of Catalunya, Campus del Baix Llobregat, Edifici D4, Esteve Terradas, 8, Castelldefels, 08860, Spain

Jordi Palacín
Department of Computer Science and Industrial Engineering, University of Lleida, Jaume II, 69, Lleida, 25197, Spain

Abstract Estimation of grapevine vigour using mobile proximal sensors can provide an indirect method for determining grape yield and quality. Of the various indexes related to the characteristics of grapevine foliage, the leaf area index (LAI) is probably the most widely used in viticulture. To assess the feasibility of using light detection and ranging (LiDAR) sensors for predicting the LAI, several field trials were performed using a tractor-mounted LiDAR system. This system measured the crop in a transverse direction along the rows of vines and geometric and structural parameters were computed. The parameters evaluated were the height of the vines (*H*), the cross-sectional area (*A*), the canopy volume (*V*) and the tree area index (*TAI*). This last parameter was formulated as the ratio of the crop estimated area per unit ground area,

using a local Poisson distribution to approximate the laser beam transmission probability within vines. In order to compare the calculated indexes with the actual values of LAI, the scanned vines were defoliated to obtain LAI values for different row sections. Linear regression analysis showed a good correlation (R^2=0.81) between canopy volume and the measured values of LAI for 1 m long sections. Nevertheless, the best estimation of the LAI was given by the *TAI* (R^2=0.92) for the same length, confirming LiDAR sensors as an interesting option for foliage characterization of grapevines. However, current limitations exist related to the complexity of data process and to the need to accumulate a sufficient number of scans to adequately estimate the LAI.

Keywords LAI · Precision viticulture · Proximal sensing · Terrestrial laser scanner · Vine vigour

Introduction

The leaf area index (LAI) is defined as the one-side leaf area per unit ground area and is probably the most widely used index to characterize grapevine vigour. In addition, LAI is spatially variable and therefore maps of vineyard leaf area could be used for many purposes such as to optimize site-specific management. In viticulture, there is also a clear need for developing on-the-go “quality” sensors. This is one of the principal objectives of precision viticulture. The aim is to be able to estimate parameters to define grape quality by direct or indirect measurement at pre-harvest or at the time of harvest. However, direct measurement of grape quality is complicated. Tisseyre et al. (2001) carried out trials with some degree of success using sensors on grape harvesting machines to determine average sugar content (refractrometry) and acidity (pH). On the

other hand, there is a well known inter-relationship between production (amount harvested), vine vigour and quality of the harvested grapes. In fact, a measure of the grapevine vigour can be obtained (Tregoat et al. 2011) from estimations of the total leaf area and/or the leaf area of the lateral shoots (Sanchez-de-Miguel 2011), which can provide another factor to be considered in indirect determinations of harvest quality and quantity (Hall et al. 2002).

It is clear that the provision of an adequate and well-exposed leaf surface affects the amount of photosynthesis and, therefore, the final synthesis and accumulation of compounds affecting grape quality (Hidalgo 2006). There are different indexes related to grapevine vigour. Among these, the total leaf area or LAI can be estimated by direct measurement which requires the use of destructive leaf sampling methods which are costly and time-consuming. Faced with this technique, vineyard leaf area can be indirectly estimated using various types of sensors (Jonckheere et al. 2004) in what has been called indirect non-contact LAI measurement. Experiments have been carried out using plant canopy analyzers (e.g. LAI-2000, LI-COR Inc., Lincoln, NE, USA) to indirectly estimate the LAI in viticulture (Grantz and Williams 1993; Tregoat et al. 2001; Johnson and Pierce 2004). This kind of sensor measures the light extinction through the foliage. However, a general trend towards underestimating LAI due to foliage clumping (Jonckheere et al. 2004; Johnson and Pierce 2004), and the requirement for an above canopy reference reading in order to get accurate LAI estimations are known weaknesses of the LAI-2000 approach. The use of ceptometer devices and hemispherical photographs has also been referenced (López-Lozano et al. 2009).

Another possibility is the use of ground-based sensors to get information about the geometry and/or structure of the canopy (López-Lozano et al. 2009; Rosell et al. 2009b; Llorens et al. 2011). Specifically, laser sensors have been tested in fruit orchards (apple and pear) (Walklate et al. 2002; Palacín et al. 2007; Rosell et al. 2009a; Sanz et al. 2011), in citrus (Wei and Salyani 2004; Lee and Ehsani 2009) and in grapevine, in which in addition to laser sensors (Arnó et al. 2006; Rosell et al. 2009b; Llorens et al. 2011), radiometric sensors mounted on tractors were used (Goutouly et al. 2006; Drissi et al. 2009; Mazzetto et al. 2010). As an alternative to optical sensors, ultrasonic sensors (US) have been used to estimate LAI in cereals (Scotford and Miller 2004) and measure canopy volume in different crops: fruit trees (Giles et al. 1988; Solanelles et al. 2006; Escolà et al. 2011), grapevines (Gil et al. 2007; Llorens et al. 2011) and citrus (Tumbo et al. 2002; Schumann and Zaman 2005; Zaman and Schumann 2005). However, more accurate measurements are obtained using laser sensors due to the lower vertical sampling resolution of US (Lee and Ehsani 2009).

Remote sensing, using satellite and airborne imaging systems, is another option that has also been used to estimate the LAI or to map vigour differences within vineyards (Johnson et al. 2001; Hall et al. 2002). For example, Johnson et al. (2003) obtained a significant correlation (R^2 = 0.72) between the estimated leaf area per vine using the Normalized Difference Vegetation Index (NDVI) calculated from satellite images and the leaf area per vine obtained by direct and indirect measurements on the ground. However, it is also known that the relationship between LAI and NDVI varies over time and requires a specific calibration according to the different growth stages of the crop. Johnson et al. (2003) also pointed out the difficulty of remote estimation of LAI in vineyards due to the spatial discontinuity of this crop in which leaves are

concentrated over long stems and cover a relatively small percentage of the ground surface. Vegetation present between rows (such as vegetative cover or weeds) further complicates the correct interpretation of reflectance data in the images. In addition, remote sensing LAI estimates are usually validated by handheld LAI instruments as they operate similarly and are also affected by foliage clumping. By contrast, terrestrial laser scanners (TLS) operate laterally penetrating the canopy from different angles, and therefore the sensor validation requires actual LAI values obtained by destructive leaf sampling methods. The terrestrial sensors that provide NDVI values (or other appropriate vegetation indices) operate similarly to airborne and satellite sensors. The *GreenSeeker* sensor (Trimble Agriculture Division, Westminster, CO, USA) uses bands that sample in the visible red (660 nm) and near-infrared (770 nm) portions of the electromagnetic spectrum (Goutouly et al. 2006; Drissi et al. 2009), and the *CropCircle* sensor (Holland Scientific Inc., Lincoln, NE, USA) uses bands that sample in the visible orange (595 nm) and near-infrared (880 nm) portions of the electromagnetic spectrum (Stamatiadis et al. 2010). Such ground-based sensors are more widely accepted in the domain of precision agriculture (viticulture) for measuring ground level crop reflectance.

The continuous evaluation of the canopy in vineyards is undoubtedly an important objective in precision viticulture. A laser sensor (using Light Detection And Ranging or LiDAR technology) has been the instrument chosen in this research work to reliably estimate LAI and canopy density in grapevines. We have discarded ultrasonic sensors due to their low vertical sampling resolution (Tumbo et al. 2002; Wei and Salyani 2004) and reflectance ground-based sensors due to their relatively poor ability to estimate and encompass the entire canopy (Drissi et al. 2009). In fact, there exist

some interesting LiDAR applications in agriculture demonstrating the potential of laser scanning systems. For example, Ehlert et al. (2008, 2010) and Saeys et al. (2009) used a laser system for measuring crop biomass and crop density in cereals, respectively. Gebbers et al. (2011) also used laser sensors to map LAI in broadacre crops. Measurement of wood volume by means of a LiDAR sensor has been proposed by Keightley and Bawden (2010) for grapevine biomass analysis. More recently, field characterization of olive trees has also been possible using TLS systems (Moorthy et al. 2011). As far as the possible applications in horticulture, LiDAR sensor has become an excellent device to reliably quantify tree geometric characteristics (Rosell et al. 2009b; Sanz et al. 2011). The matter is the large amount of data provided and what are the most suitable procedures to analyse and extract valuable information.

Wei and Salyani (2005) and Lee and Ehsani (2009) developed a laser based measurement system and associated algorithms specifically designed to estimate the canopy volume in citrus trees. Likewise, Palacín et al. (2007) and Rosell et al. (2009b) also suggested the measurement of canopy volume in orchards to subsequently make possible the estimation of total leaf area by an allometric relationship between both parameters. In vineyard, Llorens et al. (2011) also proposed a similar procedure. However, these methods are very sensitive to the distance between the laser sensor travel line and the tree row line (Palleja et al. 2010). Measurement errors could appear when the sensor deviates from the path, usually in asymmetrically shaped trees, if there are no specific corrections. On the other hand, the use of such allometric equations may be limited to specific conditions since volume/leaf area relationship may depend in turn on the crop, stand density and canopy structure.

Faced with all these methods of measuring canopy volume, Walklate et al. (2002) obtained several canopy parameters by analysing data from a LiDAR sensor using a probability based model. In the study presented herein, the geometric and structural parameters mentioned in the work of Walklate et al. (2002) in orchards were obtained, reviewed and validated for the specific case of estimating the LAI in vineyards. It is known that sunlight is of vital importance in viticulture (Smart 1985), and light interception through the canopy is normally described using light extinction probability models. The Poisson model has been used in the work presented here to analyze the performance of LiDAR measurements of foliage characteristics in vineyards. Ultimately, the goal is to check the operation and feasibility of a ground laser scanner in viticulture as a crop sensor, making possible a reliable LAI estimation in grapevines. In this sense, the developed LiDAR system has to be able to estimate foliage area for both symmetric and asymmetric tree shapes regardless of the side of the row from which the LiDAR reading is performed. The method should also be simple, fast and non-destructive, without requiring the use of allometric relationships. Additionally, it has to allow the estimation of foliar density within vines.

Materials and methods

Laser scanner

LiDAR sensors operate based on the measurement of the time-of-flight (TOF) of an infrared laser pulse (Lee and Ehsani 2008). In our case, the time the pulse takes to travel from the sensor to the canopy of vines and back. For each interception with a vine leaf, the sensor determines the radial distance (r) between the intercepted point and the sensor position and the angular coordinate (θ) of this intercepted point according to an adequate reference system (Fig. 1). The laser beam is sequentially emitted in different

191 directions within a vertical plane according to a given angular resolution. Therefore,
192 each scanning cycle performs a two-dimensional fan-shaped scan (Fig. 2a), so that vines
193 are scanned in a vertical cross-sectional plane. Field data are organized as a matrix of
194 polar coordinates (r, θ) of intercepted points with the position of the sensor as the origin
195 of coordinates. Thus, each vertical scan produces a matrix of data and the displacement
196 of the LiDAR sensor along the row gives several scans with their corresponding polar
197 coordinate matrices. The LiDAR sensor used in this study was a low-cost general-
198 purpose LMS-200 model (SICK AG, Waldkirch, Germany) with an accuracy of ±15
199 mm over a range up to 8 m, with an angular scanning range of 100º or 180º (according
200 to the characteristics of the vegetation) and an angular resolution of 1º. The MultiScan
201 program developed in MATLAB (MATrix LABoratory, The MathWorks Inc., Natick,
202 Mass., USA) was used to control the scanner, acquire data and subsequently process the
203 information. Data transfer from the sensor to a laptop was done via the RS-232
204 protocol. This external communication finally limited the scanning sampling frequency
205 up to 12 scans/s (that resulted in a horizontal scanning resolution of 2.3 cm row
206 length/scan at a speed of 1 km/h). The scanner and mounting are shown in Figure 1 and
207 Table 1 shows the basic specifications of the LMS-200 scanner provided by the
208 manufacturer.
209
210 **Fig. 1** LMS-200 scanner (left) and mounting used in the field trials (right) (Rosell et al.
211 2009b)
212
213 **Table 1** LMS-200 LiDAR sensor specifications

Wavelength (nm)	905
Maximum measurement distance (m)	8 (mm-mode), 80 (cm-mode)
Scanning range (º) (selectable)	180 (0º to 180º) and 100 (40º to 140º)
Angular resolution (º) (selectable)	0.25º, 0.5º and 1º
Scanning time (ms/cycle)	53, 26 and 13 at 0.25º, 0.5º and 1º, respectively
Precision (mm)	±15 (mm mode), ±40 (cm mode)
Weight (kg)	4.5
Dimensions (mm)	185 (width) x 156 (length) x 210 (height)

214

215

216 Data analysis

217 The LiDAR sensor generated data (polar coordinates) according to the scanner's
218 reference system shown in Figure 2a. Thus, it was assumed that the axis *Ox* was parallel
219 to the ground and directed towards the interior of the canopy, that the *Oy* axis was
220 perpendicular to the ground and that the *Oz* axis was parallel to the ground and in the
221 direction in which the LiDAR sensor moved. With this arrangement, the origin *O*
222 (LiDAR) corresponded to the centre of the semicircle of the LiDAR scan and all the
223 points intercepted by the laser beam in each semicircular scan were in the *Oxy* plane
224 (Fig. 2a). The provided (r, θ) values were r as the distance between the reference origin
225 *O* and the intercepted vegetation, and θ as the angle between the *Oy* axis and the
226 direction of the laser beam (clockwise). As the sensor moved relative to the crop (*Oz*
227 axis) (Fig. 2b), it carried out several vertical scans keeping an approximately constant
228 height from the ground, H_g.

229

230 For the subsequent analysis of the data, the interception points of the whole
231 scanned volume along the *Oz* axis (Fig. 2c) were projected onto a two-dimensional grid
232 of polar cells in the *Oxy* plane (Fig. 2d), so the overall projected cross-section of the
233 canopy volume was divided into cells with equal angle increments of $\Delta\theta = 3^\circ$ and equal
234 radial increments of Δr = 100 mm. The height of the sensor from the ground is denoted
235 by H_g and d_t is the distance used to exclude intercepted points at ground and trunk level
236 whose Cartesian coordinates in height (*Oy*) satisfy: $y < -(H_g - d_t)$.

237

238 **Fig. 2** a) Coordinate system of the sensor for a complete single scan (0º to 180º). b)
239 Simulated vertical scans along the row. c) Intercepted points generated by several scans

along a row (1 m in length) seen in the *Oxy* plane. d) Projection of the scans along the *Oz* axis onto a two-dimensional grid of polar cells in the *Oxy* plane

A diagram showing a two-dimensional polar cell (*k*, *j*) is also shown in Figure 2d, where '*k*' refers to the angular position of the cell from the *Oy* axis (clockwise), and '*j*' refers to the radial position (distance) relative to the LiDAR sensor. For a specific polar cell, the number of interceptions, $\Delta n_{k,j}$, occurring between the laser beam and the presence of vegetative material in its path within the cell should satisfy the following expression:

$$\Delta n_{k,j} = n_{k,j} - n_{k,j+1} \quad [1]$$

where $n_{k,j}$ is the number of laser beams reaching the entrance side of the polar cell (*k*, *j*) and $n_{k,j+1}$ is the number of beams that cross the exit side of the cell and, therefore, enter the next cell. To apply equation [1], it was necessary to know the number of beams entering the first cells, that is the cells close to the LiDAR sensor (*k*, *j* = 1). This value could be easily established by taking into account that the number of scans carried out over a section of 4 m in the row was between 163 and 191, the angular resolution of the sensor was 1º, and the angle increment $\Delta\theta$ of the cells was 3º. So, typical number of entering beams ranged from 489 to 573. Readings from the LiDAR sensor were finally structured according to two data matrices: the interception matrix ($\Delta n_{k,j}$) and the matrix of beams entering each cell ($n_{k,j}$). In other words, the information about the crop was reduced to a two-dimensional distribution over the *Oxy* plane of the laser beam interception with the crop canopy, and a two-dimensional distribution on the same plane describing the attenuation that the laser beam undergoes on passing through the crop canopy. The crop vegetation parameters shown in Table 2 were obtained from the two aforementioned matrices.

Table 2 Vegetative parameters of vines computed from the LiDAR sensor data

Parameter	Formulae	Notation
Tree height [a] (H) (m)	$H = H_g + \mathbf{max}\left(r_j \, \delta_{k,j} \sin\left(\frac{\pi}{2} - \theta_k \right) \right)$	H_g is the height of the LiDAR above the ground (m) and r_j (m) and θ_k (rad) are the polar coordinates of the cell (k, j).
Cross-sectional area (A) (m^2)	$A = \Delta\theta \, \Delta r \sum_{k=1}^{K} \sum_{j=1}^{J_k} r_j \, \delta_{k,j}$	This is the cross section projected onto the Oxy plane, where r_j is the polar distance (m), $\Delta\theta$ is the angle increment (rad) and Δr is the radial increment (m).
Canopy volume (V) (m^3)	$V = \frac{\Delta z}{1000} \sum_{i=1}^{N} A_i$	This is the sum of the unit volumes from each scan, where A_i is the cross-sectional area of each scan i, Δz is the width (mm) between two consecutive scans, and N the number of scans carried out.
Tree area index (TAI) (dimensionless)	$TAI = -\frac{\Delta\theta}{W} \sum_{k=1}^{K} \sum_{j=1}^{J_k} r_j \, \delta_{k,j} \ln\left(1 - \frac{\Delta n_{k,j}}{n_{k,j}} \right)$	Using the Poisson model to determine the probability of the laser beam's transmission within vines, the TAI index is formulated as the ratio between the crop detected area by the LiDAR sensor and the ground area. W (m) is the row spacing.

[a] In all the formulae, the presence or absence of foliage in each cell was indicated by the function $\delta_{k,j}$ taking a value of $\delta_{k,j} = 1$ when the coefficient $\Delta n_{k,j} / n_{k,j}$ is greater or equal to 0.01, and a value of $\delta_{k,j} = 0$ when the coefficient is less than 0.01 (Walklate et al. 2002).

In the most recent scientific literature (Llorens et al. 2011), the estimation of canopy volume has been proven to be a useful method for the indirect determination of leaf area in vineyards. In this study, the total canopy volume was obtained by adding up the volumes of the individual slices (scans), as shown in Table 2. This methodology differs from that used by Walklate et al. (2002), where the canopy volume is calculated from the cross-sectional area (A) and the row scanned length.

Faced with the parameters related to geometry of the crop (H, A and V), the TAI is the most related parameter to the leaf density of the crop. In obtaining this parameter, and similarly to Walklate et al. (2002), firstly it was considered (Fig. 2d) that the

probability of transmission of laser beam in a generic cell (*k*, *j*) could be established by dividing the amount of beams at the output ($n_{k,j+1}$) and the amount of beams at the entrance ($n_{k,j}$),

$$T_{k,j} = 1 - \frac{\Delta n_{k,j}}{n_{k,j}} \quad [2]$$

and, secondly, this probability could be approximated by the Poisson probability model when sufficiently small distances Δr, and random spatial distribution of the canopy are considered (Walklate 1989),

$$T_{k,j} = \exp\left(-\Delta r \cdot a_{k,j}\right). \quad [3]$$

Thus, it was possible to assign to each cell (*k*, *j*) a particular value of the parameter $a_{k,j}$ (local area density of the crop [L^{-1}]), which could be considered as the ratio of the area detected by the LiDAR in the direction Δr and the volume of the corresponding cell. Combining the expressions [2] and [3], the value of the local area density for a cell (*k*, *j*) was obtained from LiDAR data as

$$a_{k,j} = -\frac{1}{\Delta r} \ln\left(1 - \frac{\Delta n_{k,j}}{n_{k,j}}\right). \quad [4]$$

Adding the vegetation detected by the LiDAR sensor in each cell and dividing by the total ground area on which the scan was performed, *TAI* is finally obtained using the equation shown in Table 2.

Field trials

The field trials were carried out in a vineyard (Merlot) in Raimat (Lleida, Spain). They consisted of four trials at four different growth stages of the vines. In each trial a 4-m

306 long row section was scanned corresponding to three consecutive vines (LAI zone)
307 which were subsequently manually defoliated according to the sections shown in the
308 diagram in Figure 3. LAI was then determined for 1 m row lengths taking individual
309 sections 1, 2, 3 and 4 (Fig. 3). LAI for 2-m row length sections was obtained by
310 combining sections 1 and 2 and sections 3 and 4, while LAI for 4-m row length was
311 obtained by combining all the sections. A planimeter (Delta-T Devices Ltd., Cambridge,
312 UK) was used in combination with a gravimetric method correlating fresh weight of
313 leaves and leaf area. LAI was determined for both left and right sides of the row
314 separately and as an average for the total row width. The LAI zone (Fig. 3) was scanned
315 twice from each side of the row, at a speed of approximately 1 km/h, with the sensor at
316 1.60 m above ground level, obtaining a total of 4 readings per row scanned length. The
317 establishment of the LAI zones was possible using reference stands 0.55-m wide and
318 1.10-m high, located 0.40 m from the center of the row as shown in Figure 4. For the
319 experiments (Table 3), the LMS-200 was operated in the mm-mode and scanned the
320 vines in different scanning ranges (depending on the development of the crop) with an
321 angular resolution of 1º. The ground surface of the travel path for the tractor was
322 relatively even and, to avoid measurement errors, field trials were carried out in calm
323 wind conditions.
324

325 **Fig. 3** Diagram of the scanning procedure over a row using LiDAR sensor (left), and
326 defoliation sections 1, 2, 3 and 4 (1-m length) of the LAI zone (right). Thus, either eight
327 values of the LAI were obtained when left and right row sides were considered
328 separately (shaded area), and four values when the row was considered as a whole
329

330 **Table 3** Field trials

Date	Block	Vines	Scanning range (º)	Number of scans (1-m long section)
5/10/2005	I	15, 16 and 17	60 - 180	42
6/6/2005	II	21, 22 and 23	40 - 160	46 - 48
7/7/2005	III	24, 25 and 26	40 - 160	41
8/24/2005	IV	18, 19 and 20	40 - 160	46

Fig. 4 Left-side view of block III with vines with foliage (left) and right-side view of defoliated vines of the same block III (right)

Finally, the relationship between LAI and the LiDAR parameters was evaluated by regression analysis according to linear models of the following type:

$$LAI = \hat{\beta}_0 + \hat{\beta}_1 \cdot LiDAR \quad [5]$$

where *LAI* is the Leaf Area Index (m^2/m^2), *LiDAR* is the considered vegetative parameter (expressed in the corresponding units) and $\hat{\beta}_0$ and $\hat{\beta}_1$ are the estimates of the model parameters obtained by the method of least squares. Regression analysis was performed using Microsoft Excel 2002 and the goodness of fit was checked by the coefficient of determination (R^2) and the contrast of the regression (model significance).

Results and discussion

LiDAR performance in measuring LAI and leaf area density

In general, when the leaf area (LAI) of the vines increased, there was a proportional increase in the values of the parameters obtained by the LiDAR sensor. However, the *TAI* was the parameter that showed the greatest ability to predict the LAI. Specifically, with defoliation sections of 1 m, the *TAI* parameter was able to explain 92 % of the variability of LAI, compared with 81% that was explained by the canopy volume. Both regression models estimate the LAI of the total width of the row, i. e. regardless of the side of the row from which the sensor readings are made. The cross-sectional area and the tree height parameters also showed interesting results (Table 4), but they are slightly poorer given the R^2 results (0.72 and 0.62, respectively).

LiDAR parameters were different (although with slight variation) when the sensor scannings were made from different sides (left or right) of the row. Probably, as suggested by Walklate et al. (2002), these differences were due to the asymmetry of the vegetative structure of the vines. This result raised the question of whether it was appropriate to use the LiDAR sensor only from one side to estimate the total leaf area of the row or, by contrast, it was more convenient to formulate a model that was specifically applicable to estimate the leaf area of only half the width of the row (right or left sides). Thus, in a second analysis, four additional regression models were obtained with the aim of investigating the relationship between leaf area of each half of the row-width (or partial LAI) and the LiDAR parameters obtained using readings from the corresponding side of the row (1-m long). By considering the LAI of the right and left sides of the row separately, a greater number of data was handled (32 LAI values and 64 values of each LiDAR parameter). Once again, the canopy volume (R^2 = 0.71) and the tree area index (R^2 = 0.83) were the parameters showing the best estimation of LAI (Table 4). On the other hand, the vine height did not seem to be a good option when estimating grapevine leaf area (R^2 = 0.54).

Leaf area index prediction for longer lengths was another option (Table 4). The models obtained for sections of 2 m and 4 m showed even better results, essentially attributable to the lower amount of points used. Except for the tree height parameter, higher R^2 values were obtained (between 0.86 and 0.99), confirming the excellent performance of the LiDAR sensor. However, results for section lengths of 1 m were probably more reliable as they were based on more robust models (with higher number of observations/points).

It is clear that the *TAI* showed itself to be a valuable parameter for estimating the LAI. To bring together one overall model that would be valid for canopy sections of 1-m, 2-m and 4-m lengths, and also to estimate the total, or partial, leaf area of a row, LAI could be estimated with the following average equation:

$$LAI = 1.2646 * TAI - 0.1935 \quad (R^2 = 0.99) \qquad [6]$$

which was obtained by regression analysis of the predicted LAI values (or fit LAI values) using the four linear models shown in Table 4 for canopy sections of 1 m, 2 m and 4 m. Equation [6] has an obvious advantage because the LAI of vines could be estimated from scanning only one of the sides of the row. This feature is especially interesting as it reduces the mapping and scanning time required for a field.

Table 4 Statistical analysis of simple linear regression models for predicting the LAI in vineyards

Estimation of LAI of the total width of the row (sections of 1-m long)						
LiDAR parameter	**Model significance**	**R^2**	**Coefficient* $\hat{\beta}_0$**	**Coefficient* $\hat{\beta}_1$**	**C.I. 95 % for $\hat{\beta}_1$**	
					Lower	**Upper**
Tree height, *H* (m)	<0.0001	0.62	-3.8104 (0.4972)	2.1790 (0.2158)	1.7476	2.6103
Cross-sectional area, *A* (m^2)	<0.0001	0.72	-0.1931 (0.1140)	1.8982 (0.1497)	1.5990	2.1975
Canopy volume, *V* (m^3)	<0.0001	0.81	-0.6685 (0.1193)	11.2666 (0.7032)	9.8608	12.6723
Tree area index, *TAI*	<0.0001	0.92	-0.2329 (0.0566)	1.3014 (0.0491)	1.2032	1.3996
Estimation of LAI of only half the width of the row (right or left sides, sections of 1-m long)						
LiDAR parameter	**Model significance**	**R^2**	**Coefficient* $\hat{\beta}_0$**	**Coefficient* $\hat{\beta}_1$**	**C.I. 95 % for $\hat{\beta}_1$**	
					Lower	**Upper**
Tree height, *H* (m)	<0.0001	0.54	-3.7416 (0.5844)	2.1490 (0.2536)	1.6420	2.6560
Cross-sectional area, *A* (m^2)	<0.0001	0.66	-0.2149 (0.1337)	1.9279 (0.1756)	1.5770	2.2789
Canopy volume, *V* (m^3)	<0.0001	0.71	-0.6681 (0.1535)	11.2640 (0.9049)	9.4552	13.0728
Tree area index, *TAI*	<0.0001	0.83	-0.2444 (0.0873)	1.3118 (0.0759)	1.1602	1.4635
Estimation of LAI of the total width of the row (sections of 2-m long)						
LiDAR parameter	**Model significance**	**R^2**	**Coefficient* $\hat{\beta}_0$**	**Coefficient* $\hat{\beta}_1$**	**C.I. 95 % for $\hat{\beta}_1$**	
Tree height, *H* (m)	<0.0001	0.57	-3.3512 (0.7183)	1.9577 (0.3084)	1.3278	2.5876
Cross-sectional area, *A* (m^2)	<0.0001	0.87	-0.2515 (0.1047)	1.6362 (0.1140)	1.4034	1.8690
Canopy volume, *V* (m^3)	<0.0001	0.86	-0.7379 (0.1430)	5.8418 (0.4229)	4.9781	6.7054

Tree area index, *TAI*	<0.0001	0.95	-0.1741 (0.0603)	1.2395 (0.0522)	1.1329	1.3461

Estimation of LAI of the total width of the row (sections of 4-m long)

LiDAR parameter	**Model significance**	**R^2**	**Coefficient*** $\hat{\beta}_0$	**Coefficient*** $\hat{\beta}_1$	**C.I. 95 % for** $\hat{\beta}_1$	
Tree height, *H* (m)	<0.0001	0.74	-3.8960 (0.8131)	2.1764 (0.3466)	1.4331	2.9198
Cross-sectional area, *A* (m^2)	<0.0001	0.96	-0.2875 (0.0801)	1.4440 (0.0750)	1.2831	1.6048
Canopy volume, *V* (m^3)	<0.0001	0.98	-1.0398 (0.0870)	3.3759 (0.1290)	3.0992	3.6527
Tree area index, *TAI*	<0.0001	0.99	-0.1226 (0.0331)	1.2057 (0.0288)	1.1439	1.2674

***** Standard errors of β_0 and β_1 estimators' are shown in parentheses.

The final proposed model [6] may be questionable according to two basic concepts. First, LiDAR does not distinguish between green and non-green elements which makes the *TAI* a parameter conceptually similar to Plant Area Index (PAI) as proposed in Moorthy et al. (2011), and second, actual canopy foliage is not uniform or randomly distributed due to vegetation structure (Weiss et al. 2004). In fact, Moorthy et al. (2011) obtain the PAI after calculating a clumping index that, unlike the *TAI*, considers nonrandom distribution of vegetation. Furthermore, the *TAI* parameter can vary in leafless vines that have different wooden structure. Therefore, estimation of LAI based on the Poisson model using the *TAI* parameter will provide estimates of an effective leaf area index (L^{eff}) as suggested by Weiss et al. (2004). The term "effective LAI" is useful for describing optical LAI estimates using methods that do not distinguish leaves from other plant elements, and are unable to compensate for non-random positioning of leaves within the canopy (Jonckheere et al. 2004). Underestimation errors caused by clumping and the inherent row structure of vineyards are therefore expected when comparing *TAI* derived from LiDAR measurements with the actual LAI value measured with destructive sampling (Johnson and Pierce 2004). Testing the effect of clumping has been possible by forcing the linear regression model according to the expression:

$$LAI = \hat{\beta} \cdot TAI = \hat{\beta} \cdot L^{eff} \quad [7]$$

where L^{eff} is the 'effective' leaf area index (m^2/m^2) computed as *TAI*, and β (>1, if clumping effect is true) is the model's coefficient. Table 5 shows the obtained results. As expected, in both cases (whole and half row width) the *TAI* parameter underestimates the true value of LAI by about 10 %, confirming the irregular but non-random distribution of leaves in vineyard. However, the sensitivity of *TAI* to LAI is evident (Tables 4 and 5) and no saturation occurs for higher values of LAI (figures not shown). *TAI* is therefore a valid parameter for the estimation of LAI, and this result also confirms the findings of López-Lozano et al. (2009) in which the Poisson model can be applied for LAI < 3 (which are typical values in vineyards) using LiDAR to provide lateral observations of the vines from perpendicular scans to the rows.

Table 5 Linear regression models between the LAI and the 'effective' leaf area index (L^{eff}) for 1-m long sections of crop vegetation

Whole-row width			Half-row width		
Coefficient $\hat{\beta}$	R^2	RMSE	Coefficient $\hat{\beta}$	R^2	RMSE
1.1082	0.90	0.1509	1.1091	0.81	0.2191

The leaf area density is defined as the total one-side leaf area of photosynthetic tissue per unit canopy volume (Weiss et al. 2004). As already mentioned above, *TAI* is a parameter that was obtained taking into account the foliage density of the crop. The two-dimensional plot of the local density values ($a_{k,j}$) [4] should allow the visual interpretation of foliage density (or foliage distribution) detected by the LiDAR sensor within the canopy. Figure 5 shows the foliage density plots for each of the scanned blocks of 4-m length (scans accumulated over 4 m and performed from the left side of the row). The highest densities appeared to concentrate within the inner parts of the canopy and, also, with increasing LAI there was a proportional increase in *TAI* and cross-sectional area. The measurement of high values of local density in some cells of the lower parts of the canopy could be due to the presence of grapes in these zones.

Fig. 5 Grapevine foliage density of the scanned blocks (4-m row length from the left side) by plotting the values of local area density, $a_{k,j}$ [4]

Required number of accumulated scans to derive LAI

After verifying the suitability of the tree area index for estimating the leaf area index, the analysis of foliage variability could be addressed by analyzing the variability of *TAI* along the row. Figure 6a shows the values of *TAI* for each of the scans performed in block I (early stages of crop cycle). It is observed that the variability of *TAI* (and, presumably, the leaf area) along the row was evident and, more importantly, repeated readings (in blue) of the same block showed very similar results to those obtained in the first scan (in red). These results confirmed the suitability of LiDAR sensors to accurately and repeatedly detect and quantify vineyard canopies.

Fig. 6 *TAI* values in two repeated readings (red and blue) from the left side of the row, cv. Merlot, 10 May, 2005 (Block I): a) Individual values of *TAI* for each of the 170 scans performed; b) Accumulated *TAI* scans along the row (4-m length); c and d) Cumulative values of *TAI* in lengths of 2 m and 1 m, respectively

The remaining issue was to determine the required row length that should be scanned for an optimal use of the LiDAR sensor. At first, data available were the values of *TAI* based on the projection of scans made over a certain row length (in our case, 4 m, 2 m and 1 m). However, further calculation of the accumulated values of *TAI*, as scans were progressively overlaid and projected, provided very interesting information about the operation and use of LiDAR technology in field conditions. Figure 6 shows the evolution of *TAI* with the accumulation of LiDAR scans. Specifically, it shows the cumulative values for different row lengths (b-4 m, c-2 m, d-1 m) for the vegetation block tested on 10 May, 2005 (Block I). Graphical analysis of the block (Fig. 6) reveals

that the value of *TAI* showed some stabilization with higher number of scans accumulated. This trend was more evident in sections (row lengths) of 4 m and 2 m, probably contributing to smooth the *TAI* values and to mask the spatial variability at these scales. However, in sections of 1 m the values of the last cumulative *TAI* presented greater differences from one to another section, being the detection of foliage variability along the row more effective in this spatial scale. Faced with the possibility of using the LiDAR scanner as a sensor for mapping LAI at parcel level, we suggest calculating the value of *TAI* based on scans accumulated in 1 m length sections in each of the sampling areas. In our working conditions, this means calculating the *TAI* after 40-50 accumulated scans.

The assessment of leaf area variability along a row can be addressed through the use of LiDAR technology. However, further research is needed to confirm the LiDAR as a reliable crop sensor. If the good results of this study were confirmed, LiDAR sensors could have several and interesting applications in viticulture. For instance, LiDAR sensors could be an excellent device for predicting grape yield and quality related parameters when the spatial covariance between vigor, yield and quality is acceptable. In this sense, they would solve the need for sensors for indirect and continuous monitoring of grape quality, similarly to how grape yield monitors work.

Conclusions

LiDAR sensors with the configuration proposed in this research provide a feasible method to monitor within-field leaf area variability and can have several applications in precision viticulture. Among the parameters obtained from the LiDAR sensor data, the canopy volume and, above all, tree area index have shown a higher ability to estimate

leaf surface (or LAI) in vineyards. Furthermore, estimation of leaf area corresponding to the total width of the row can be done by scanning with LiDAR from only one side of the row. In other cases, *TAI* can also be used to estimate leaf area of half the width of the row corresponding to the scanned side, i.e. to estimate the leaf area between the canopy and the average plane defined by the trunks of vines. As grapevine leaf surface is variable along the row, the use of LiDAR sensors for obtaining reliable LAI maps should also consider the section row length to be scanned in each sampling area. Specifically, scanning section row lengths of 1 m (40 to 50 scans) is the option we recommend. Scanned lengths of 2 m and 4 m provided *TAI* values that are somewhat smoothed since they account for a greater row length. This would mask the spatial variability detected at these scales. The main difficulties with the technology are the non-random distribution of leaves (which moves away from the Poisson model) and the presence of leaves and other non-green vegetative elements within the canopy. Since the intensity of the returned laser beam is also provided by some LiDAR sensors, future research could explore the applicability of this information to better characterize grapevine canopies.

Acknowledgements This research was funded by ERDF (European Regional Development Fund) and the Spanish Ministry of Science and Education (Agreement No. AGL2002-04260-C04-02, and acronym PULVEXACT, and Agreement No. AGL2007-66093-C04-03, and acronym OPTIDOSA). Likewise, the authors wish to thank the Agricultural Division of Codorníu for providing the vineyard field where trials were conducted.

References

518 Arnó, J., Vallès, J. M., Llorens, J., Blanco, R., Palacín, J., Sanz, R., et al. (2006).
519 Ground laser scanner data analysis for Leaf Area Index (LAI) prediction in orchards and
520 vineyards. In: *Book of Abstracts of the AgEng 2006 Conference* (pp. 311-312). Bonn,
521 Germany: VDI Verlag GmbH.
522 Drissi, R., Goutouly, J. P., Forget, D., & Gaudillere, J. P. (2009). Nondestructive
523 measurement of grapevine leaf area by ground Normalized Difference Vegetation
524 Index. *Agronomy Journal, 101*(1), 226-231.
525 Ehlert, D., Heisig, M., & Adamek, R. (2010). Suitability of a laser rangefinder to
526 characterize winter wheat. *Precision Agriculture, 11*(6), 650-663.
527 Ehlert, D., Horn, H. J., & Adamek, R. (2008). Measuring crop biomass density by laser
528 triangulation. *Computers and Electronics in Agriculture, 61*(2), 117-125.
529 Escolà, A., Planas, S., Rosell, J. R., Pomar, J., Camp, F., Solanelles, F., et al. (2011).
530 Performance of an ultrasonic ranging sensor in apple tree canopies. *Sensors, 11*(3),
531 2459-2477.
532 Gebbers, R., Ehlert, D., & Adamek, R. (2011). Rapid mapping of the leaf area index in
533 agricultural crops. *Agronomy Journal, 103*(5), 1532-1541.
534 Gil, E., Escolà, A., Rosell, J. R., Planas, S., & Val, L. (2007). Variable rate application
535 of plant protection products in vineyard using ultrasonic sensors. *Crop Protection,*
536 *26*(8), 1287-1297.
537 Giles, D. K., Delwiche, M. J., & Dodd, R. B. (1988). Electronic measurement of tree
538 canopy volume. *Transactions of the ASAE, 31*(1), 264-272.
539 Goutouly, J. P., Drissi, R., Forget, D., & Gaudillère, J. P. (2006). Characterization of
540 vine vigour by ground based NDVI measurements. In: *Proceedings of the VI*
541 *International Terroir Congress* (pp. 237-241). Bordeaux, France.

Grantz, D. A., & Williams, L. E. (1993). An empirical protocol for indirect measurement of leaf area index in grape (*Vitis vinifera* L.). *HortScience, 28*(8), 777-779.

Hall, A., Lamb, D. W., Holzapfel, B., & Louis, J. (2002). Optical remote sensing applications in viticulture-A review. *Australian Journal of Grape and Wine Research, 8*, 36-47.

Hidalgo, J. (2006). *La calidad del vino desde el viñedo (The quality of wine from the vineyard)*. Madrid, Spain: Mundi-Prensa.

Johnson, L. F., Bosch, D. F., Williams, D. C. & Lobitz, B. M. (2001). Remote sensing of vineyard management zones: Implications for wine quality. *Applied Engineering in Agriculture, 17*(4), 557-560.

Johnson, L. F. & Pierce, L. L. (2004). Indirect measurements of leaf area index in California north coast vineyards. *HortScience, 39*(2), 236-238.

Johnson, L. F., Roczen, D. E., Youkhana, S. K., Nemani, R. R., & Bosch, D. F. (2003). Mapping vineyard leaf area with multispectral satellite imagery. *Computers and Electronics in Agriculture, 38*(1), 33-44.

Jonckheere, I., Fleck, S., Nackaerts, K., Muys, B., Coppin, P., Weiss, M., et al. (2004). Review of methods for in situ leaf area index determination: Part I. Theories, sensors, and hemispherical photography. *Agricultural and Forest Meteorology, 121*(1-2), 19-35.

Keightley, K. E., & Bawden, G. W. (2010). 3D volumetric modelling of grapevine biomass using Tripod LiDAR. *Computers and Electronics in Agriculture, 74*(2), 305-312.

Lee, K. H., & Ehsani, R. (2008). Comparison of two 2D laser scanners for sensing object distances, shapes, and surface patterns. *Computers and Electronics in Agriculture, 60*(2), 250-262.

567 Lee, K. H., & Ehsani, R. (2009). A laser scanner based measurement system for
568 quantification of citrus tree geometric characteristics. *Applied Engineering in*
569 *Agriculture, 25*(5), 777-788.
570 Llorens, J., Gil, E., Llop, J., & Escolà, A. (2011). Ultrasonic and LIDAR sensors for
571 electronic canopy characterization in vineyards: advances to improve pesticide
572 application methods. *Sensors, 11*(2), 2177-2194.
573 López-Lozano, R., Baret, F., García de Cortázar-Atauri, I., Bertrand, N., & Casterad, M.
574 A. (2009). Optimal geometric configuration and algorithms for LAI indirect estimates
575 under row canopies: The case of vineyards. *Agricultural and Forest Meteorology,*
576 *149*(8), 1307-1316.
577 Mazzetto, F., Calcante, A., Mena, A., & Vercesi, A. (2010). Integration of optical and
578 analogue sensors for monitoring canopy health and vigour in precision agriculture.
579 *Precision Agriculture, 11*(6), 636-649.
580 Moorthy, I., Miller, J. R., Jimenez Berni, J. A., Zarco-Tejada, P., Hu, B., & Chen, J.
581 (2011). Field characterization of olive (*Olea europaea* L.) tree crown architecture using
582 terrestrial laser scanning data. *Agricultural and Forest Meteorology, 151*(2), 204-214.
583 Palacín, J., Pallejà, T., Tresánchez, M., Sanz, R., Llorens, J., Ribes-Dasi, M., et al.
584 (2007). Real-time tree-foliage surface estimation using a ground laser scanner. *IEEE*
585 *Transactions on Instrumentation and Measurement, 56*(4), 1377-1383.
586 Palleja, T., Tresanchez, M., Teixido, M., Sanz, R., Rosell J. R., & Palacin, J. (2010).
587 Sensitivity of tree volume measurement to trajectory errors from a terrestrial LIDAR
588 scanner. *Agricultural and Forest Meteorology, 150*(11), 1420-1427.
589 Rosell, J. R., Llorens, J., Sanz, R., Arnó, J., Ribes-Dasi, M., Masip, J., et al. (2009a).
590 Obtaining the three-dimensional structure of tree orchards from remote 2D terrestrial
591 LIDAR scanning. *Agricultural and Forest Meteorology, 149*(9), 1505-1515.

592 Rosell, J. R., Sanz, R., Llorens, J., Arnó, J., Escolà, A., Ribes-Dasi, M., et al. (2009b). A
593 tractor-mounted scanning LIDAR for the non-destructive measurement of vegetative
594 volume and surface area of tree-row plantations: A comparison with conventional
595 destructive measurements. *Biosystems Engineering, 102*(2), 128-134.
596 Saeys, W., Lenaerts, B., Craessaerts, G. & De Baerdemaeker, J. (2009). Estimation of
597 the crop density of small grains using LiDAR sensors. *Biosystems Engineering, 102*(1),
598 22-30.
599 Sanchez-de-Miguel, P., Junquera, P., de la Fuente, M., Jimenez, L., Linares, R., Baeza,
600 P., & Lissarrague, J. R. (2011). Estimation of vineyard leaf area by linear regression.
601 *Spanish Journal of Agricultural Research, 9*(1), 202-212.
602 Sanz, R., Llorens, J., Escolà, A., Arnó, J., Ribes-Dasi, M., Masip, J., et al. (2011).
603 Innovative LIDAR 3D dynamic measurement system to estimate fruit-tree leaf area.
604 *Sensors, 11*(6), 5769-5791.
605 Schumann, A. W., & Zaman, Q. U. (2005). Software development for real-time
606 ultrasonic mapping of tree canopy size. *Computers and Electronics in Agriculture,*
607 *47*(1), 25-40.
608 Scotford, I. M., & Miller, P. C. H. (2004). Estimating Tiller Density and Leaf Area
609 Index of Winter Wheat using Spectral Reflectance and Ultrasonic Sensing Techniques.
610 *Biosystems Engineering, 89*(4), 395-408.
611 Smart, R. E. (1985). Principles of grapevine canopy microclimate manipulation with
612 implications for yield and quality. A review. *American Journal of Enology and*
613 *Viticulture, 36*(3), 230-239.
614 Solanelles, F., Escolà, A., Planas, S., Rosell, J. R., Camp, F., & Gràcia, F. (2006). An
615 electronic control system for pesticide application proportional to the canopy width of
616 tree crops. *Biosystems Engineering, 95*(4), 473-481.

Stamatiadis, S., Taskos, D., Tsadila, E., Christofides, C., Tsadilas, C. & Schepers, J. S. (2010). Comparison of passive and active canopy sensors for the estimation of vine biomass production. *Precision Agriculture, 11*(3), 306-315.

Tisseyre, B., Mazzoni, C., Ardoin, N., & Clipet, C. (2001). Yield and harvest quality measurement in precision viticulture – Application for a selective vintage. In: G. Grenier & S. Blackmore (Eds.), *Proceedings of the 3rd European Conference on Precision Agriculture* (pp. 133-138). France, Agro Montpellier.

Tregoat, O., Ollat, N., Grenier, G., & Van Leeuwen, C. (2001). Etude comparative de la précision et de la rapidité de mise en œuvre de différentes méthodes d'estimation de la surface foliaire de la vigne. *Journal International des Sciences de la Vigne et du Vin, 35*(1), 31-39. [In French].

Tumbo, S. D., Salyani, M., Whitney, J. D., Wheaton, T. A., & Miller, W. M. (2002). Investigation of laser and ultrasonic ranging sensors for measurements of citrus canopy volume. *Applied Engineering in Agriculture, 18*(3), 367-372.

Walklate, P. J. (1989). A laser scanning instrument for measuring crop geometry. *Agricultural and Forest Meteorology, 46*(4), 275-284.

Walklate, P. J., Cross, J. V., Richardson, G. M., Murray, R. A., & Baker, D. E. (2002). Comparison of different spray volume deposition models using LIDAR measurements of apple orchards. *Biosystems Engineering, 82*(3), 253-267.

Wei, J., & Salyani, M. (2004). Development of a laser scanner for measuring tree canopy characteristics: Phase 1. Prototype development. *Transactions of the ASABE, 47*(6), 2101-2107.

Wei, J., & Salyani, M. (2005). Development of a laser scanner for measuring tree canopy characteristics: Phase 2. Foliage density measurement. *Transactions of the ASABE 48*(4), 1595-1601.

Weiss, M., Baret, F., Smith, G. J., Jonckheere, I., & Coppin, P. (2004). Review of methods for in situ leaf area index (LAI) determination. Part II. Estimation of LAI, errors and sampling. *Agricultural and Forest Meteorology, 121*(1-2), 37-53.

Zaman, Q. U., & Schumann, A. W. (2005). Performance of an ultrasonic tree volume measurement system in commercial citrus groves. *Precision Agriculture, 6*(5), 467-480.

Fig. 1 LMS-200 scanner (left) and mounting used in the field trials (right) (Rosell et al. 2009b)

Fig. 2 a) Coordinate system of the sensor for a complete single scan (0º to 180º). b) Simulated vertical scans along the row. c) Intercepted points generated by several scans along a row (1-m long) seen in the *Oxy* plane. d) Projection of the scans along the *Oz* axis onto a two-dimensional grid of polar cells in the *Oxy* plane

Fig. 3 Diagram of the scanning procedure over a row using LiDAR sensor (left), and defoliation sections 1, 2, 3 and 4 (1-m length) of the LAI zone (right). Thus, either eight values of the LAI were obtained when left and right row sides were considered separately (shaded area) and four values when the row was considered as a whole

Fig. 4 Left-side view of block III with vines with foliage (left) and right-side view of defoliated vines of the same block III (right)

Fig. 5 Grapevine foliage density of the scanned blocks (4-m row length from the left side) by plotting the values of local area density, $a_{k,j}$ [4]

Fig. 6 *TAI* values in two repeated readings (red and blue) from the left side of the row, cv. Merlot, 10 May, 2005 (Block I). a) Individual values of *TAI* for each of the 170 scans performed. b) Accumulated *TAI* scans along the row (4-m length). c and d) Cumulative values of *TAI* in lengths of 2 m and 1 m, respectively

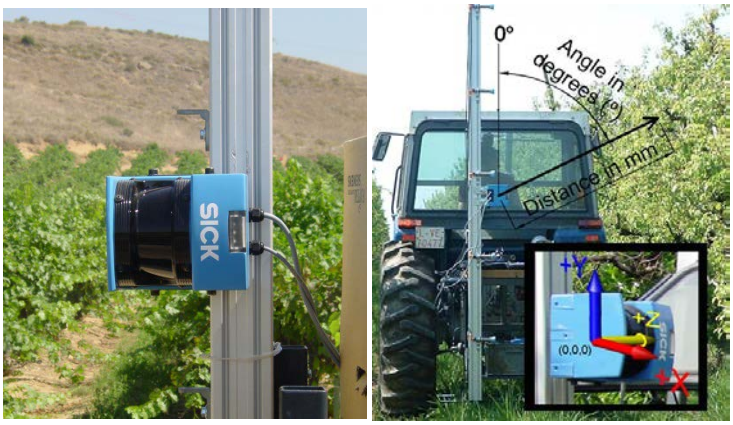
SICK
0°
Angle in degrees (θ)
Distance in mm
+Y
+Z
+X
(0,0,0)

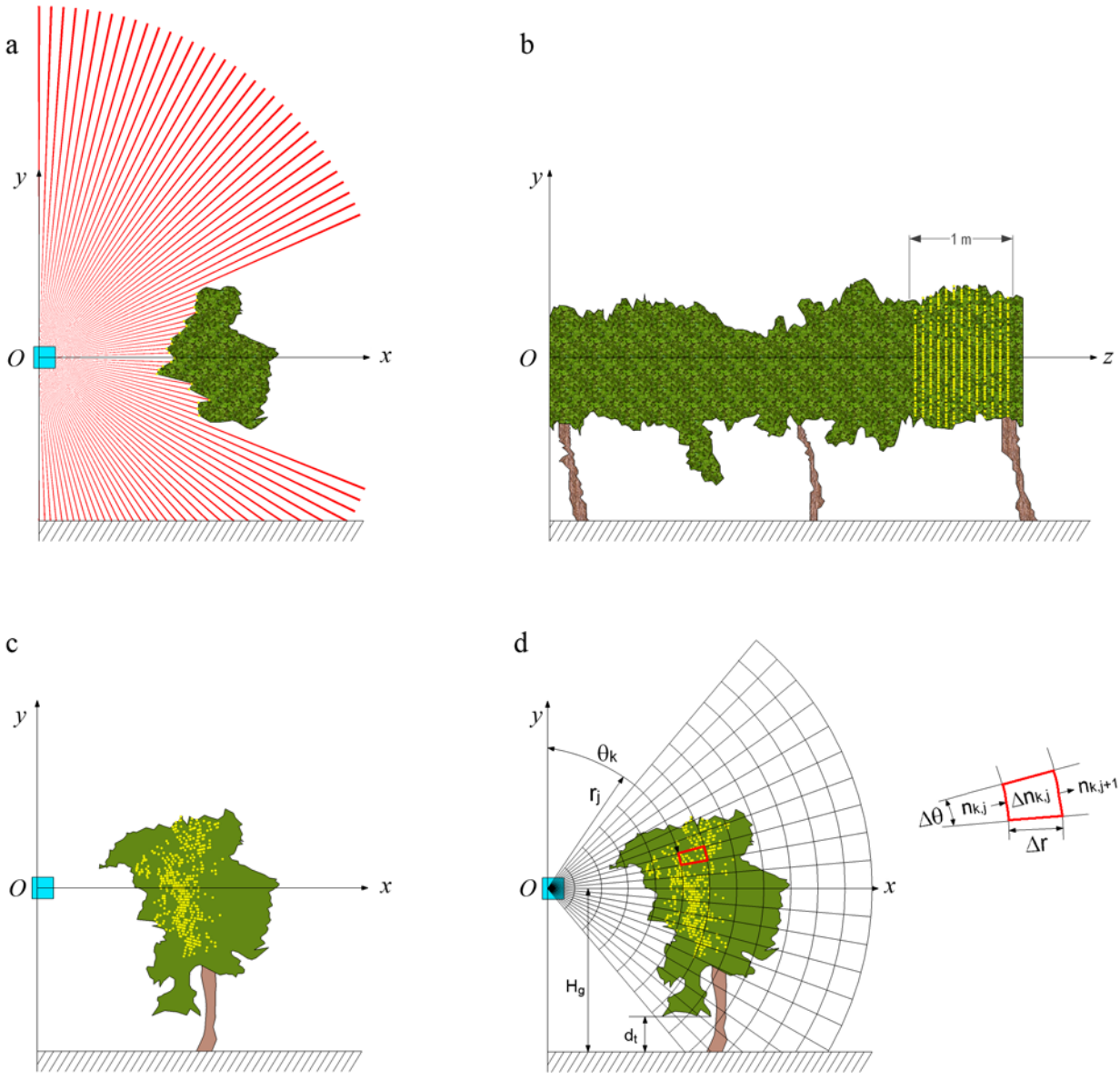
a
y
O
x
b
y
1 m
O
z
c
y
O
x
d
y
θk
rj
O
x
Hg
dt
Δθ
nk,j
Δnk,j
nk,j+1
Δr

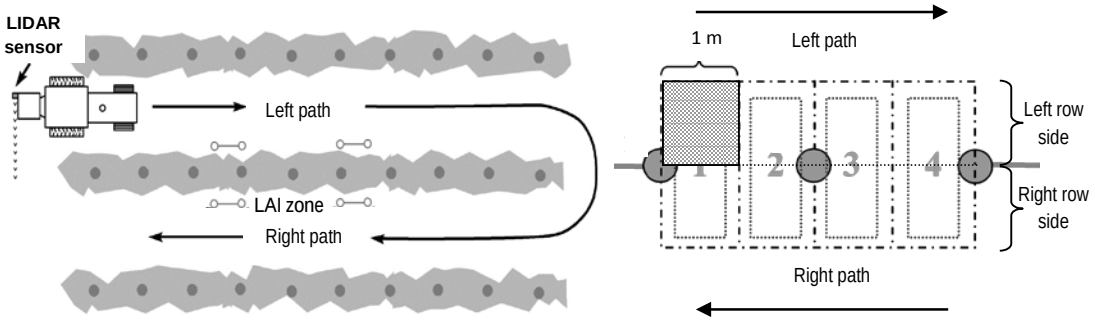
LIDAR sensor
Left path
LAI zone
Right path
1 m
Left path
1
2
3
4
Left row side
Right row side
Right path


May 10 field trial, LAI = 0.5033

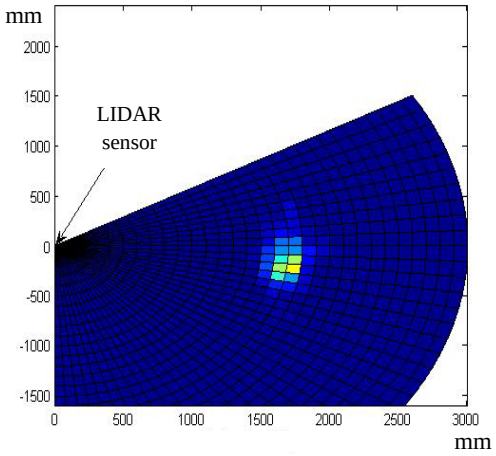

Cross-sectional area, A = 0.599 m^2
Tree area index, TAI = 0.532

June 6 field trial, LAI = 1.2646

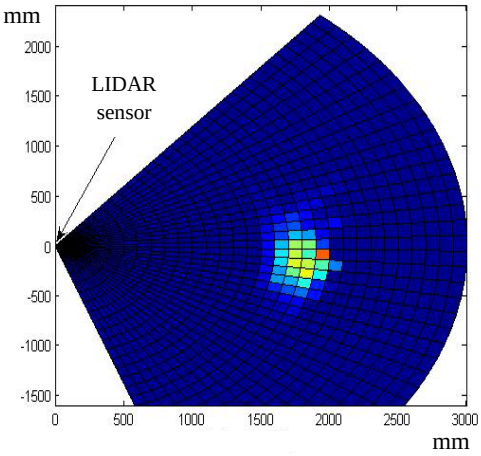

Cross-sectional area, A = 1.017 m^2
Tree area index, TAI = 1.162

July 7 field trial, LAI = 1.6591

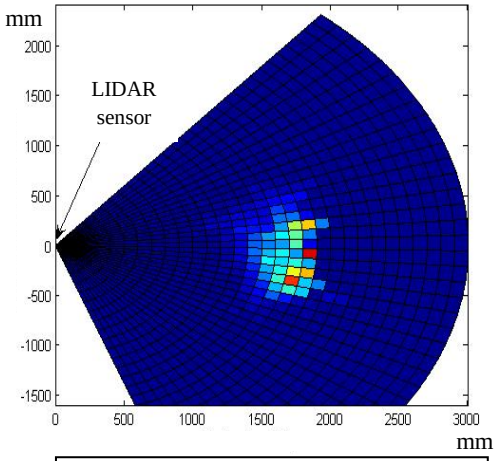

Cross-sectional area, A = 1.350 m^2
Tree area index, TAI = 1.495

August 24 field trial, LAI = 1.3601

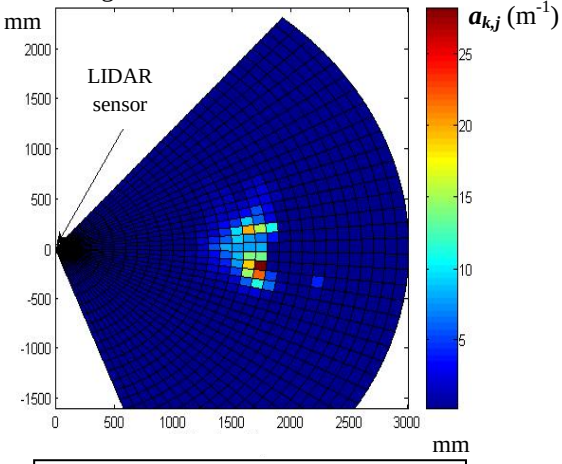

Cross-sectional area, A = 1.138 m^2
Tree area index, TAI = 1.189

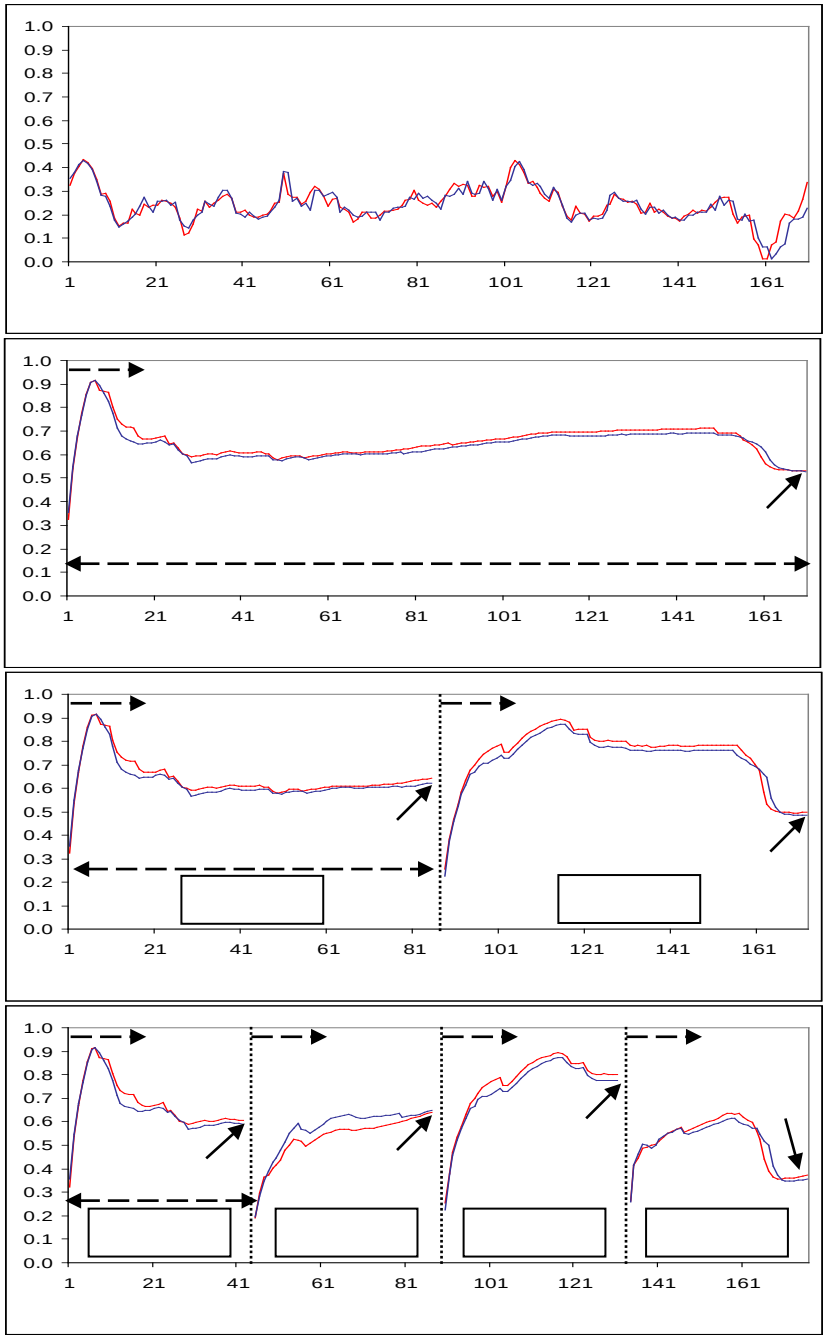
1.0
0.9
0.8
0.7
0.6
0.5
0.4
0.3
0.2
0.1
0.0
1
21
41
61
81
101
121
141
161